CRYSTALLIZATION CHARACTERISTICS OF B_2O_3 AND TiO_2-BEARING GLASSY FLUORIDE-FREE MOLD FLUXES

Z. Wang [a, b, c, d, *], Q.-F. Shu [e], K.-C. Chou [e]

[a]* Institute of Process Engineering, Chinese Academy of Sciences, State Key Laboratory of Multiphase Complex Systems, Beijing, P.R. China
[b]* University of Chinese Academy of Sciences, School of Chemical Engineering, Beijing, P.R. China
[c]* Nanjing IPE Institute of Green Manufacturing Industry, Nanjing, P.R. China
[d]* Innovation Academy for Green Manufacture, Chinese Academy of Sciences, Beijing, P.R. China
[e] University of Science and Technology Beijing, State Key Laboratory of Advanced Metallurgy, Beijing, P.R. China

Abstract

To explore the effects of TiO_2 and/or B_2O_3 on crystallization of the glassy fluoride-free slag film near the copper mould, the crystallization characteristics of glassy fluoride-free mold fluxes with fluoride being substituted by TiO_2 and/or B_2O_3 were investigated using X- ray diffraction (XRD), scanning electron microscope (SEM) and differential thermal analysis (DTA) techniques. The glass forming ability index (K_{gl}) of the glassy fluoride-free mold fluxes was studied using Hruby's method. The XRD and SEM analysis show that $Ca_2Al_2SiO_7$, $CaTiO_3$ and $CaSiO_3$ are the dominant crystals of this fluoride-free mold fluxes system. With the content of TiO_2 increasing from 0 to 7%, the crystallization of $Ca_2Al_2SiO_7$ and $CaSiO_3$ are inhibited and the formation of $CaTiO_3$ is also weak, so crystallization tendency of the glassy fluoride-free mold fluxes weakens. But as TiO_2 content reaches 10%, the crystallization tendency strengthens because of the strong crystallization of $CaTiO_3$. An increase of B_2O_3 inhibits the crystallization of calcium silicate, so it weakens the crystallization tendency of the glassy fluoride-free mold fluxes. The crystallization processes of the studied fluoride-free mold fluxes correspond to the surface crystallization mechanism. This research provides important reference for further investigation on the heat transfer behavior of the TiO_2 and B_2O_3-bearing slag between copper mould and slab to evaluate the feasibility of B_2O_3 and TiO_2-bearing fluoride-free mold fluxes.

Keywords: Fluoride-free mold fluxes; Crystallization; Slag; Glass forming ability index; Surface crystallization; TiO_2

1. Introduction

Mold flux is an indispensable material in the continuous casting process. It helps to lubricate steel shell to prevent sticking against the mold surface and control the heat transfer to achieve uniform shell [1-7]. The stability of the continuous casting process and the surface quality of products are restricted to good performance of the above functions, which are closely related to the physio-chemical properties of the mold flux, such as viscosity, melting temperature, crystallization behavior [4-11]. And the implementation of the above mentioned functions is bound up with the existence of fluorides in traditional mold fluxes, which plays significant roles in adjusting physio-chemical properties of the mold fluxes. However, the fluorides can lead to erosion to continuous caster, pollution of environment, acidification of the cooling water, human health hazard, and a series of other harmful influences [6, 12-16]. Thus, there is a pressing need for fluoride-free mold fluxes, and the investigation on it has become a research area of interest.

Previous studies show that adding B_2O_3 and /or TiO_2 to mold fluxes without fluoride can adjust the properties of the slag to make it have similar characteristics with the traditional fluoride containing mold fluxes [5, 6, 10, 13-16]. On one hand, the addition of TiO_2 to mold fluxes without fluoride can ensure the crystallization of mold fluxes to make sure that the fluoride-free mold fluxes show similar heat transfer performance with the traditional fluoride containing mold fluxes [2, 5, 6, 10, 13, 17]. Also, as amphoteric oxide, TiO_2 can influence the viscosity of fluoride-free mold fluxes obviously [13], so that help to control the lubrication performance. Besides, B_2O_3, as an effective

fluxing agent to lower the melting point of mold fluxes, has been taken into consideration for being added to mold fluxes to adjust the viscosity or melting properties of slag [5, 13-19]. Or a new crystalline phase of $Ca_{11}Si_4B_2O_{22}$ in fluorine-free mold fluxes formed by the addition of B_2O_3 shows a great potential to replace the cuspidine phase in traditional mold fluxes [17, 19]. Therefore, B_2O_3 and TiO_2 are potential to replace the fluoride in traditional mold fluxes, and fluoride-free mold fluxes bearing B_2O_3 and /or TiO_2 is the promising substitutes. So it is absolutely essential to investigate the properties of mold fluxes simultaneously containing B_2O_3 and TiO_2 to develop the optimal fluoride-free mold fluxes.

According to survey performed by the present author, investigations on the properties of mold fluxes containing both B_2O_3 and TiO_2 are limited [16, 20-25]. The present authors investigated the crystallization of molten mold fluxes containing both B_2O_3 and TiO_2 and explored the effects of B_2O_3 and TiO_2 on incubation time for crystallization of molten fluxes [24]. However, besides molten layer, there is glass layer in the gap between steel shell and mold wall [3]. And the crystallization of glassy mold fluxes, i.e. devitrification of glassy mold fluxes, is also important to heat transfer between steel shell and mold. According to Watanabe et al [26, 27], mold fluxes can inevitably absorb some heat released from the solidification of liquid steel, which produces reheating to the mold fluxes. This reheating process could lead to the crystallization of glassy slag film near the copper mold, which changes crystalline layer thickness and surface roughness of solidified mold fluxes, and thereby has great effect on horizontal heat transfer and lubrication. So it would be essential to carry out the research on crystallization characteristics of glassy mold fluxes simultaneously containing B_2O_3 and TiO_2 to examine the feasibility of B_2O_3 and TiO_2-bearing fluoride-free mold fluxes.

In this work, the crystallization characteristic of B_2O_3 and TiO_2-bearing fluoride-free mold fluxes in glassy state has been investigated. Crystals precipitating from the studied glassy mold fluxes with variable TiO_2 and B_2O_3 content were identified by X-ray diffraction (XRD) and scanning electron microscope (SEM) analysis, and the crystallization mechanisms were revealed. The influences of TiO_2 and B_2O_3 on crystallization tendency of B_2O_3 and TiO_2-bearing fluoride-free mold fluxes were examined by analyzing characteristic temperatures for crystallization of the glassy fluoride-free mold fluxes determined by differential thermal analysis (DTA).

2. Experimental
2.1 Sample Preparation

Analytical grade CaO, SiO_2, Al_2O_3, MgO, TiO_2, Na_2CO_3 and H_3BO_3 (from Sinopharm Chemical

Reagent Co., Ltd) were taken as raw materials, with Na_2CO_3 and H_3BO_3 being substitutes for Na_2O and B_2O_3, respectively. Table 1 presents the chemical compositions (wt. %) of the investigated samples.

Glass samples with different TiO_2 and B_2O_3 content were prepared by the conventional melting and quenching method. After well mixed, Raw materials was taken into a platinum crucible and then melted in high temperature furnace at approximately 1573K in air atmosphere. The samples were held at 1573K for nearly 3h to make sure complete melting and homogenization. After melting, the melts were quenched by water and then bulk glass samples are formed. These glass samples are proved to be amorphous by XRD, and Figure 1 gives the XRD patterns for the quenched samples. The liquidus temperature of this system has been studied in another work of our team [28], and it is showed that the liquidus temperatures of all the samples are far blow 1573K. So when the samples were heated to 1573K and held for 3 h, it is completely melted and there is definitely no crystal formed. The XRD results in Figure 1 are in accordance with the results of liquidus temperature study.

2.2 Differential Thermal Analysis

The glass samples were pulverized into powder (less than 0.74μm) for DTA measurement. For each

Table 1. *Chemical compositions of experimental samples /wt%*

Sample Name	R=w(CaO)/w(SiO$_2$)	Al$_2$O$_3$	MgO	Na$_2$O	TiO$_2$	B$_2$O$_3$
No.1-0%TiO$_2$	1	7	2	10	0	5
No.2-3%TiO$_2$	1	7	2	10	3	5
No.3-5%TiO$_2$-5%B$_2$O$_3$	1	7	2	10	5	5
No.4-7%TiO$_2$	1	7	2	10	7	5
No.5-10%TiO$_2$	1	7	2	10	10	5
No.6-0%B$_2$O$_3$	1	7	2	10	5	0
No.7-3%B$_2$O$_3$	1	7	2	10	5	3
No.8-7%B$_2$O$_3$	1	7	2	10	5	7
No.9-10%B$_2$O$_3$	1	7	2	10	5	10

sample, about 30mg glass powder was taken into a platinum crucible to be subjected to the differential thermal analysis using Netzsch STA 449C TG-DTA calorimeter at a heating rate of 10K/min. During the whole measurement process, Argon was used as a shielding gas. α-Al$_2$O$_3$ was used as a reference material.

2.3 X-ray Diffraction Analysis

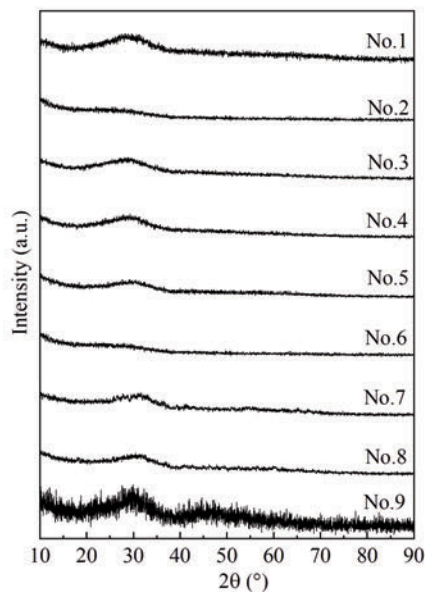The glass samples were heated in a Pt-crucible, held for approximately 4 hours at each exothermic peak temperature obtained by DTA curves and then

Figure 1. *The XRD patterns for the quenched glass samples*

quenched in air. Then each of the heat treated samples was subjected to XRD analysis to identify the products of crystallization. The XRD measurement was performed using a MAC M21XRHF22 (21KW) X-ray diffractometer with Cu Ka radiation.

2.4 Scanning Electron Microscope Measurement

The bulk glass samples were heated in a Pt-crucible, held for approximately 4 hours at each exothermic peak temperature obtained by DTA curves and then quenched in air. Then each of these heat treated samples was embedded with resin, rubbed with fine sandpaper and polished with polishing paste. The surface of each sample was experienced carbon spray coating. After that, the samples were subjected to scanning electron microscope (SEM) measurement using ZEISS EVO MA18 to obtain the microstructure of the crystallization products and the phases were identified by energy dispersive spectroscopy (EDS) attached to SEM analyzer.

3. Results and Discussion

Figure 2 and Figure 3 respectively presents the DTA and TG curves of glassy fluoride-free mold fluxes samples with different TiO$_2$ or B$_2$O$_3$ content. It can been seen from Figure 3 that weight loss of each sample is little, so volatilization during the DTA measurement mainly caused by Na$_2$O and B$_2$O$_3$ can be ignored and it is supposed that the chemical composition of each sample is invariable. From Figure 2, the glass transition temperatures (T$_g$), onset crystallization temperature (T$_x$), crystallization peak temperatures (T$_c$) and liquidus temperature (T$_l$) can be
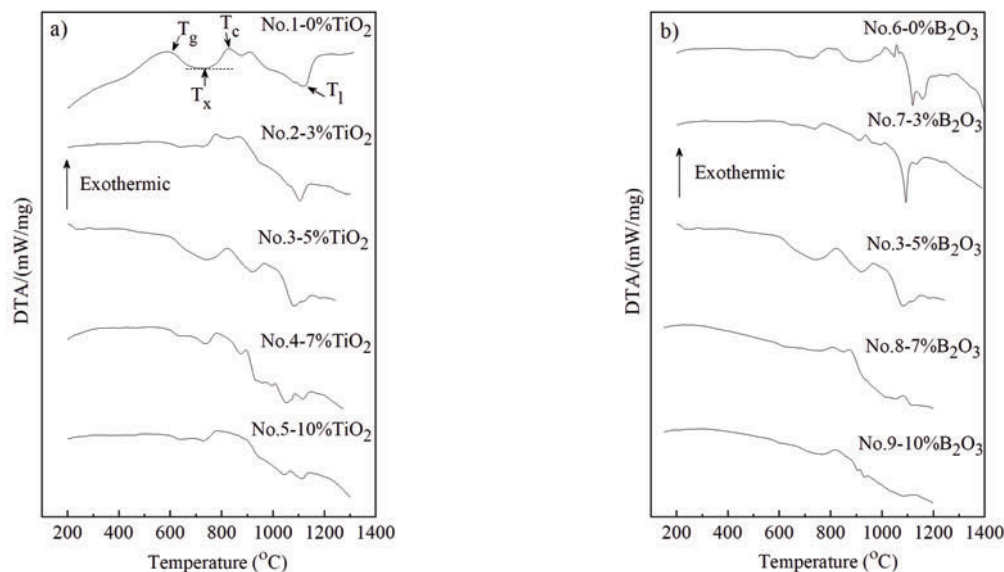

Figure 2. *DTA results of glassy fluoride-free mold fluxes with different TiO$_2$ or B$_2$O$_3$ content*

obtained. According to Boettinger et al's definition [29], acquisition method of these characteristic temperatures for crystallization process have been marked in Figure 2 a). And the corresponding characteristic temperatures for each sample can be obtained using the same method, which are summarized in Table 2.

3.1 Crystal Phase Identification

To identify the phase precipitated at each crystallization peak temperature, each heat treated samples was investigated by XRD and SEM-EDS. Figure 4, Figure 5 and Figure 6 respectively gives the XRD and SEM results for crystallized fluoride-free mold fluxes samples of $CaO-SiO_2-Al_2O_3-MgO-Na_2O-TiO_2-B_2O_3$ system.

It can be seen from Figure 4 (a) and Figure 5 that for the sample free of TiO_2, gehlenite ($Ca_2Al_2SiO_7$) and wollastonite ($CaSiO_3$) can precipitate from the slag, and with the addition of TiO_2, besides gehlenite and wollastonite, another crystal, perovskite ($CaTiO_3$), forms during the crystallization of the glassy fluoride-free mold fluxes. And the small white crystal particles in Figure 5 b), c) and e) are too small to be marked by "3", indicating the $CaTiO_3$ phase. Meanwhile, with the increase of TiO_2 content, the peaks for $CaTiO_3$ in XRD patterns (Figure 4 (a)) strengthen, and there are more crystal particles for $CaTiO_3$ in SEM-BSE pictures (Figure 5 b), c) , d) and e)). That is, the increase of TiO_2 can promote the crystallization of perovskite.

From the XRD results for samples with different B_2O_3 content in Figure 4 a), it can be seen that as the content of is low (0-3%), there form gehlenite,

dicalcium silicate (Ca_2SiO_4) and perovskite during the crystallization of the glass slag samples. But in SEM-BSE pictures (Figure 6 a), b)), it is hard to observe the gehlenite phase, because it is weak in crystallization. This may be due to that as the content of B_2O_3 is low, most of SiO_2 exists in the slag in form of (Q^0) [21], which is favorable to the precipitation of Ca_2SiO_4, so the crystallization of gehlenite is suppressed. However, with the increase of B_2O_3, on one hand, Ca^{2+} associates with boron preferentially in borosilicate slag system [30-34] so that some of CaO participates the formation of Ca-O-B bonds preferentially and there is no enough CaO to form Ca_2SiO_4; on the other hand, proportion of bridging oxygen increases, so the ratio of Q^0 decreases. These lead to the disappearance of Ca_2SiO_4, while wollastonite and more gehlenite, the formation of which could occupy more bridging oxygen, appear. Above all, with the increase of B_2O_3,

Table 2. *Characteristic temperatures of crystallization process for each fluoride-free mold fluxes sample with different TiO_2 or B_2O_3 content*

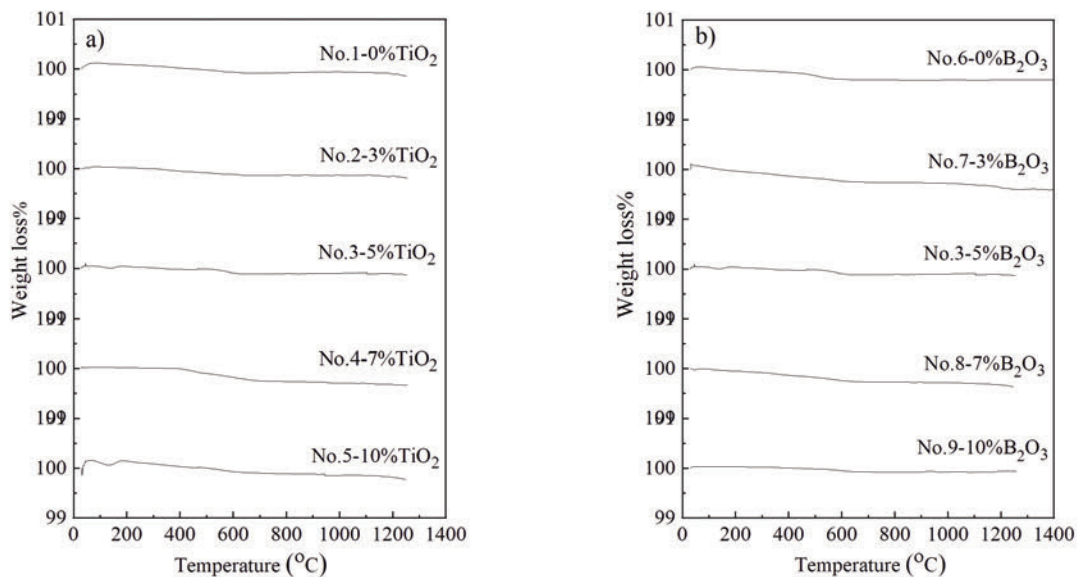| Sample Name	T_g /K	T_x /K	T_l /K
No.1-0%TiO_2	883	1012	1400
No.2-3%TiO_2	880	1013	1376
No.3-5%TiO_2-5%B_2O_3	875	1018	1388
No.4-7%TiO_2	863	1018	1390
No.5-10%TiO_2	878	993	1458
No.6-0%B_2O_3	903	1003	1532
No.7-3%B_2O_3	883	1013	1503
No.8-7%B_2O_3	863	1003	1333
No.9-10%B_2O_3	848	1038	1358

Figure 3. *TG curves of glassy fluoride-free mold fluxes with different TiO_2 or B_2O_3 content*
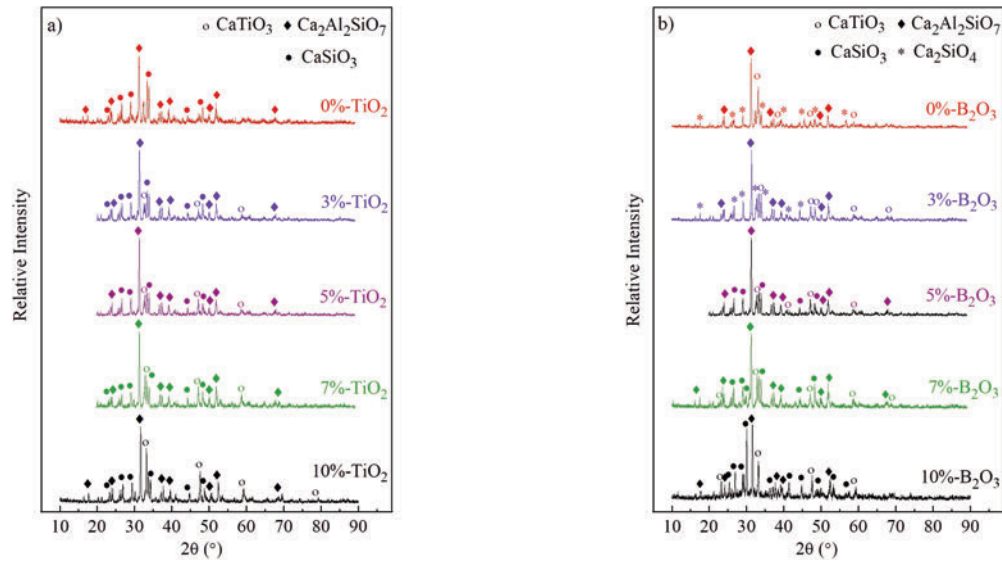
Figure 4. *XRD patterns for the crystallized fluoride-free mold fluxes with different TiO_2 or B_2O_3 content*
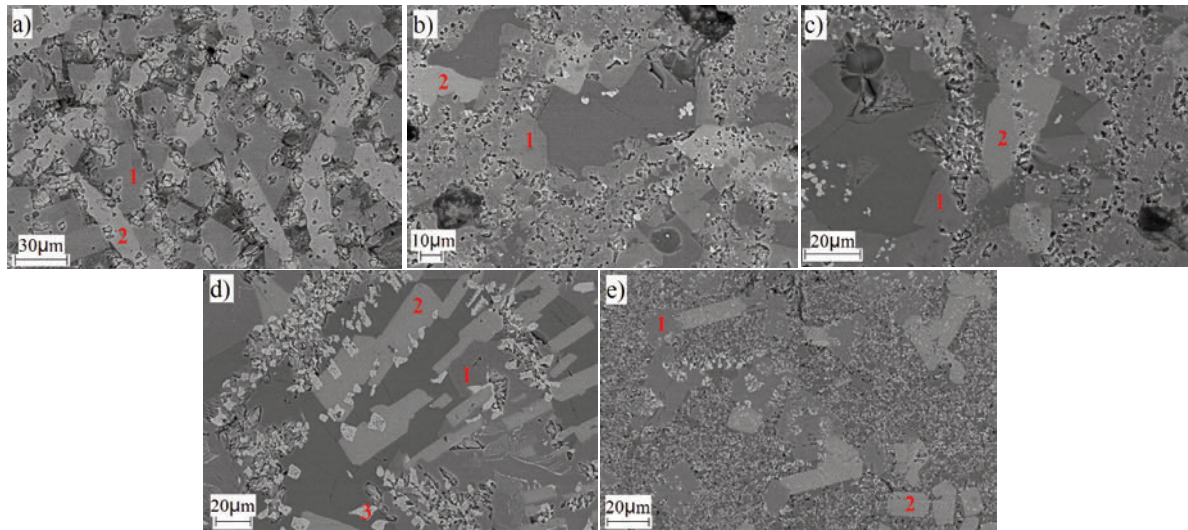

Figure 5. *SEM-BSE images for the crystallized fluoride-free mold fluxes with different TiO_2 content, a)-0% TiO_2, b)-3% TiO_2, c)-5% TiO_2, d)-7% TiO_2, e)-10% TiO_2 and 1: $Ca_2Al_2SiO_7$, 2: $CaSiO_3$, 3: $CaTiO_3$*

Ca_2SiO_4 disappears gradually, gehlenite and wollastonite form, so the primary crystal phases in the slag turn into gehlenite, wollastonite and perovskite.

Based on all the above results, the crystal phases formed in the crystallized fluoride-free mold fluxes samples of $CaO-SiO_2-Al_2O_3-MgO-Na_2O-TiO_2-B_2O_3$ system have been summarized in Table 3.

In short, $Ca_2Al_2SiO_7$, $CaTiO_3$ and $CaSiO_3$ are the dominant crystals of the investigated TiO_2 and B_2O_3-bearing fluoride-free mold fluxes. Since crystals' critical effect on horizontal heat transfer from mould to strand, the investigation on thermal resistance of slag films containing $Ca_2Al_2SiO_7$, $CaTiO_3$ and $CaSiO_3$ would be carried out in a future study.

3.2 Crystallization Mechanism

There are limited reports on the mechanism of mold fluxes crystallization from glass (devitrification of the glassy mold fluxes) [35-37]. Generally, surface crystallization mechanism has been proposed by some researchers in the study of crystallization of glassy mold fluxes [36, 37]. Mizuno et al. [37] studied the crystallization of glassy mold fluxes using light optical microscopy and laser confocal microscopy and found that crystal grains precipitated on the surface and grew toward the center of the specimen. In this study, similar phenomenon is observed. It is observed that, after being heat-treated, the surface of the sample is opaque, but the center of the sample is nearly
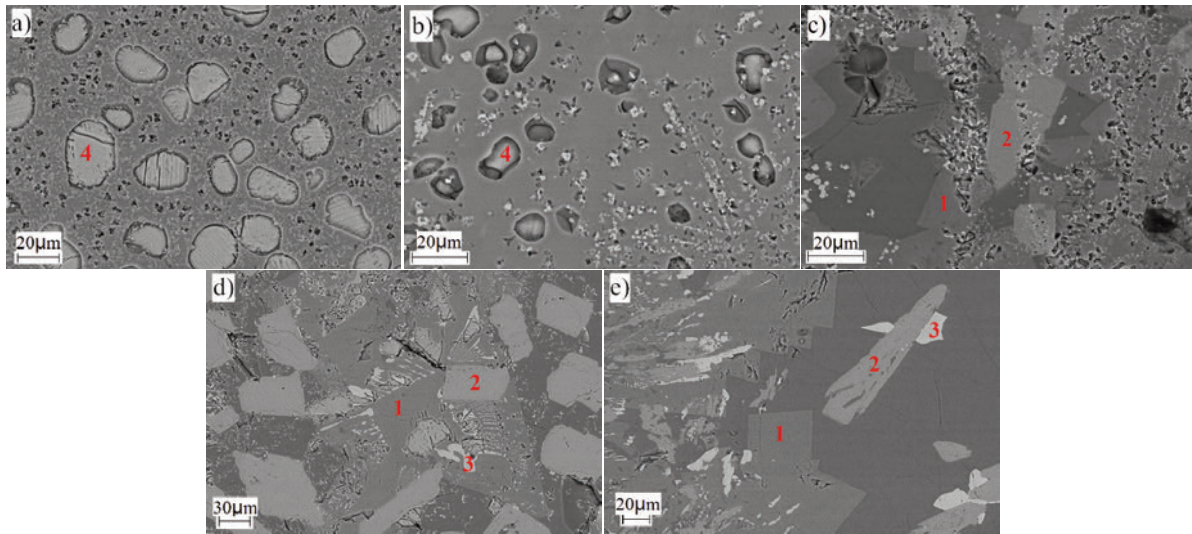
Figure 6. SEM-BSE images for the crystallized fluoride-free mold fluxes with different B_2O_3 content, a)-0% B_2O_3, b)-3% B_2O_3, c)- 5% B_2O_3, d)-7% B_2O_3, e)-10% B_2O_3 and 1: $Ca_2Al_2SiO_7$, 2: $CaSiO_3$, 3: $CaTiO_3$, 4: Ca_2SiO_4

Table 3. Crystals precipitating from the studied fluoride-free mold fluxes with different TiO_2 or B_2O_3 content

Sample Name	Crystals			
No.1-0%TiO_2	$Ca_2Al_2SiO_7$		$CaSiO_3$	
No.2-3%TiO_2	$Ca_2Al_2SiO_7$	$CaTiO_3$	$CaSiO_3$	
No.3-5%TiO_2-5%B_2O_3	$Ca_2Al_2SiO_7$	$CaTiO_3$	$CaSiO_3$	
No.4-7%TiO_2	$Ca_2Al_2SiO_7$	$CaTiO_3$	$CaSiO_3$	
No.5-10%TiO_2	$Ca_2Al_2SiO_7$	$CaTiO_3$	$CaSiO_3$	
No.6-0%B_2O_3	$Ca_2Al_2SiO_7$	$CaTiO_3$		Ca_2SiO_4
No.7-3%B_2O_3	$Ca_2Al_2SiO_7$	$CaTiO_3$		Ca_2SiO_4
No.8-7%B_2O_3	$Ca_2Al_2SiO_7$	$CaTiO_3$	$CaSiO_3$	
No.9-10%B_2O_3	$Ca_2Al_2SiO_7$	$CaTiO_3$	$CaSiO_3$	

transparent. By SEM measurement (Figure 7), it is found that there are plenty of crystal grains near the surface of the sample and the crystal phase is dense, while there is less columnar crystal grains in the center of the sample and the columnar crystal grains is nearly perpendicular to the surface. This is consistent with McMillan's description about crystallization process of glass, that is, crystals grow inwards from the glass surface and quite often they are oriented at 90° to the glass surface [38]. So it is inferred that crystallization processes of the studied fluoride-free mold fluxes correspond to the surface crystallization mechanism, which is consistent with the previous investigations on crystallization of glassy mold fluxes or glass [35-38].

3.3 Effects of TiO_2 and B_2O_3 on Crystallization of Glassy Fluoride-free Mold Fluxes

It is known that, for a silicates slag system, the more easily of glass forming, the more stable the glass and

the weaker the crystallization tendency [39]. So the crystallization tendency of the studied fluoride-free mold fluxes with changes of TiO_2 and B_2O_3 content can be examined by investigating stability of the glass from TiO_2 and B_2O_3-bearing fluoride-free mold fluxes.

Many indexes have been proposed to estimate the stability of glass, and Hruby's method has been widely accepted [39-40]. According to Hruby et al [40], the glass forming ability index (K_{gl}) is expressed as the following equation:

$$K_{gl} = \frac{T_x - T_g}{T_l - T_x} \tag{1}$$

Based on the explanation of Hruby et al [40], a short interval $T_x - T_g$ signifies that the glass contains some structural units with higher crystallization tendency, i.e., the original melt is unfavorable to the formation of glass, while a short temperature interval $T_l - T_x$ indicates that the crystalline phase, which is formed at T_x, has relatively lower melting point, that is, the original melt has relatively low solidification

temperature, i.e., it is favorable to formation of glass. Hruby suggests that $T_x - T_g$ is directly proportional to the glass-forming tendency and $T_l - T_x$ is indirectly proportional to the glass-forming tendency. It is reported that the bigger difference $T_x - T_g$ and the smaller temperature interval $T_l - T_x$ result in a greater K_{gl}, which indicates the lower tendency of crystallization and more stable for glasses [25, 41]. According to the characteristic temperatures (T_g, T_x, and T_l) in Table 2, the value of K_{gl} for each sample has been calculated and presented in Table 4.

The relationship between K_{gl} and TiO_2 content in Table 4 has been plotted in Figure 8. It can be found that the K_{gl} values of the glassy fluoride-free mold fluxes samples increase as the content of TiO_2 increases from 0 to 7%, but as the content of TiO_2 increases to 10%, K_{gl} shows an obvious decrease. That is, adding no more than 7% TiO_2 can weaken crystallization of the glassy fluoride-free mold fluxes, and as the addition of TiO_2 reaches 10%, crystallization tendency of the glassy fluoride-free mold fluxes strengthens. From the crystals formed in the slag, it can be seen that some of CaO reacts with TiO_2 to form $CaTiO_3$ with the addition
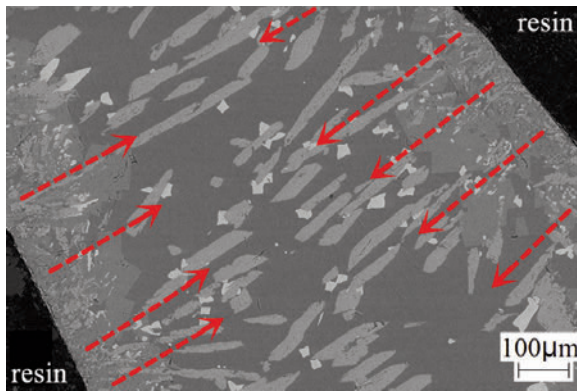
of TiO_2, so the activity of CaO which participates in the formation of gehlenite and wollastonite decreases. Consequently, the crystallization of gehlenite and wollastonite weakens. In addition, wollastonite shares a pyroxene stoichiometry, and SiO_2^{2-} (Q^2) chain is the main structure unit, which is favourable to formation of wollastonite [42]. A previous study on the same slag system by the present author has revealed that in the TiO_2-free sample, Q^2 is the dominant structure group, but increase of TiO_2 leads to the obvious decrease of Q^2 structural unit in the slag [21]. So the crystallization of wollastonite weakens. However, the crystallization of gehlenite and wollastonite are still predominant and crystallization of $CaTiO_3$ is insufficient due to the low content of TiO_2, so the crystallization ability of the mold fluxes is still controlled by the precipitation of gehlenite and wollastonite. Therefore, the crystallization tendency of the glassy fluoride-free mold fluxes weakens with TiO_2 content changing from 0 to 7%. But with the content of TiO_2 reaches 10%, the crystallization of $CaTiO_3$ is significantly enhanced, so the crystallization tendency of the glassy fluoride-free mold fluxes strengthens.

The relationship between K_{gl} and B_2O_3 content in Table 4 has been plotted in Figure 9. It can be found
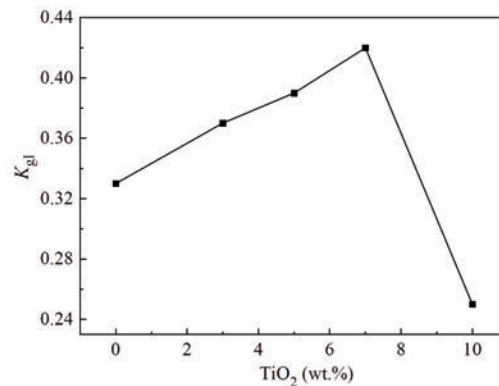

Figure 7. *Observation of surface crystallization for the studied fluoride-free mold fluxes by SEM-BSE (the arrow indicates the crystal growth direction)*

Table 4. *The K_{gl} value for each fluoride-free mold fluxes sample with different TiO_2 or B_2O_3 content*

Sample Name	K_{gl}
No.1-0%TiO_2	0.33
No.2-3%TiO_2	0.37
No.3-5%TiO_2-5%B_2O_3	0.39
No.4-7%TiO_2	0.42
No.5-10%TiO_2	0.25
No.6-0%B_2O_3	0.19
No.7-3%B_2O_3	0.27
No.8-7%B_2O_3	0.42
No.9-10%B_2O_3	0.59

Figure 8. *Relationship between the glass forming ability index (K_{gl}) and TiO_2 content*
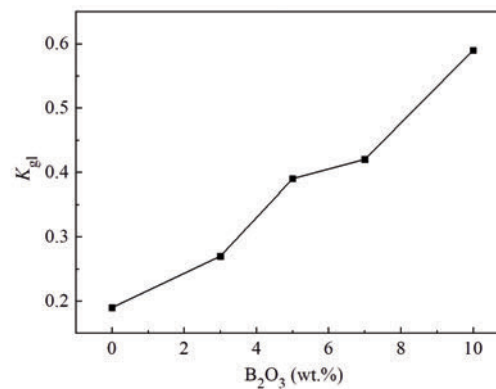

Figure 9. *Relationship between the glass forming ability index (K_{gl}) and B_2O_3 content*

that the K_{gl} values increase with the increase of B_2O_3 content. That is, B_2O_3 weakens the crystallization tendency of the glassy fluoride-free mold fluxes. On one hand, as a glass former, B_2O_3 can increases the glass-forming tendency of the investigated slag. On the other hand, as was mentioned previously, Ca^{2+} associates with boron preferentially, and with the increase of B_2O_3, some of CaO participates the formation of Ca-O-B bonds preferentially. So the crystallization of gehlenite, perovskite and wollastonite are inhibited, and thereby weakening the crystallization tendency of the glassy fluoride-free mold fluxes.

In a word, with the content of TiO_2 increasing from 0 to 7%, the glass-forming tendency of the fluoride-free mold fluxes is enhanced, while as TiO_2 content reaches 10%, the crystallization tendency of the fluoride-free mold fluxes shows an increase. B_2O_3 weakens the crystallization tendency of the glassy fluoride-free mold fluxes.

4. Conclusions

The crystallization characteristics of TiO_2 and B_2O_3-bearing fluoride-free mold fluxes have been investigated. XRD and SEM analyses showed that $Ca_2Al_2SiO_7$, $CaTiO_3$ and $CaSiO_3$ are the dominant crystals of the investigated fluoride-free mold fluxes system. Increase of TiO_2 can enhance the crystallization of $CaTiO_3$, and particularly, decrease of B_2O_3 can promote the formation of Ca_2SiO_4 as well as inhibit the crystallization of $CaSiO_3$. Due to inhibition effect of TiO_2 on crystallization of $Ca_2Al_2SiO_7$ and $CaSiO_3$, the crystallization tendency of the glassy fluoride-free mold fluxes is weakened with the content of TiO_2 increasing from 0 to 7%, and then strengthened as TiO_2 content reaches 10% because of the enhancement of $CaTiO_3$ formation. B_2O_3 weakens the crystallization tendency of the glassy fluoride-free mold fluxes. Crystallization processes of the studied fluoride-free mold fluxes correspond to the surface crystallization mechanism. This research provides important reference for further investigation on heat transfer behavior of the TiO_2 and B_2O_3-bearing slag between copper mould and slab to explore fluoride-free mold fluxes.

Acknowledgments

References

[1] M. Leng, F.F. Lai, J.L. Li, Materials, 12 (1) (2019) 62.

[2] H. Nakada, K. Nagata, ISIJ Int., 46 (3) (2006) 441-449.

[3] S.P. Gu, G.H. Wen, Z.Q. Ding, P. Tang, Q. Liu, Materials, 11 (7) (2018) 1085.

[4] K.C. Mills, A.B. Fox, ISIJ Int., 43 (10) (2003) 1479-1486.

[5] W.L. Wang, D.X. Cai, L. Zhang, ISIJ Int., 58 (11) (2018) 1957-1964.

[6] X. Qi, G.H. Wen, P. Tang, J. Non-Cryst. Solids, 354 (52/54) (2008) 5444-5452.

[7] J.Y. Park, G.H. Kim, J.B. Kim, S. Park, I. Sohn, Metal. Mater. Trans. B, 47B (2016) 2582-2594.

[8] Y.X. Gao, M. Leng, Y.F. Chen, Z.C. Chen, J.L. Li, Materials, 12 (2) (2019) 206-217.

[9] L.G. Zhu, Z.P. Yuan, Y. Xu, K.X. Zhang, Y.H. Han, High Temp. Mater. Proc., 38 (2019) 750-759.

[10] G.H. Wen, S. Sridhar, P. Tang, X. Qi, Y.Q. Liu, ISIJ Int., 47 (8) (2007) 1117-1125.

[11] W.L. Wang, P.S. Lyu, L.J. Zhou, H. Li, T.S. Zhang, JOM, 70 (7) (2018) 1248-1255.

[12] J.T. Ju, J.L. An, G.H. Ji, J. Min. Metall. Sect. B-Metall., 55 (3) B (2019) 397-404.

[13] S. Choi, D. Lee, D. Shin, S. Choi, J. Cho, J. Park, J. Non-Cryst. Solids, 345-346 (2004) 157-160.

[14] A.B. Fox, K.C. Mills, D. Lever, C. Bezerra, C. Valadares, I. Unamuno, J.J. Laraudogoitia, J. Gisby, ISIJ Int., 45 (7) (2005) 1051-1058.

[15] Z.Y. Cai, B. Song, L.F. Li, Z. Liu, X.K. Cui, Metals, 8 (10) (2018) 737-748.

[16] J. Yang, J.Q. Zhang, Y. Sasaki, O. Ostrovski, C. Zhang, D.X. Cai, Y. Kashiwaya, Metal. Mater. Trans. B, 48B (2017) 2077-2091.

[17] L. Zhang, W.L. Wang, I. Sohn, J. Non-Cryst. Solids, 511 (2019) 41-49.

[18] Z.T. Zhang, G.H. Wen, Y.Y. Zhang, Int. J. Miner. Metall. Mater., 18 (2011) 150-158.

[19] J. Wei, W.L. Wang, L.J. Zhou, D.Y. Huang, H. Zhao, F.J. Ma, Metall. Mater. Trans. B, 45 (2014) 643-652.

[20] Mccauley W.L.; Apelian D. Viscosity Characteristics of Continuous Casting Mold Fluxes. Can. Metall. Q., 20 (1981) 247-262.

[21] Z. Wang, Q.F. Shu, K.C. Chou, High Temp. Mater. Proc., 32 (3) (2013) 265-273.

[22] Z. Wang, Q.F. Shu, K.C. Chou, Steel Res. Int., 84 (8) (2013) 766-776.

[23] Z.T. Zhang, J. Li, P. Liu, J. Iron Steel Res. Int., 18 (2011) 31-37.

[24] Q.F. Shu, Z. Wang, J.L. Klug, K.C. Chou, P.R. Scheller, Steel Res. Int., 84 (11) (2013) 1138-1145.

[25] Z. Wang, Q.F. Shu, X.M. Hou, K.C. Chou, Ironmaking Steelmaking, 39 (3) (2012) 210-215.

[26] K. Watanabe, M. Suzuki, K. Murakami, H. Kondo, A. Miyamoto, T. Shiomi, Tetsu-to-Hagane´, 83 (1997) 115-120.

[27] K. Tsutsumi, T. Nagasaka, M. Hino, ISIJ Int., 39 (11) (1999) 1150-1159.

[28] Z. Wang, Q. F. Shu, K. C. Chou, Can. Metall. Quart., 52 (4) (2013) 405-412.

[29] Y.Z. Zhan, Y. Du, Y.H. Zhuang, Method for Phase

Diagram Determination (J.C. Zhao), Elsevier, Amsterdam, 2007, p. 180-191.

[30] F. Gou, G.N. Greaves, W. Smith, R. Winter, J. Non-Cryst. Solids, 293-295 (2001) 539-546.

[31] Y. Miura, H. Kusano, T. Nanba, S. Matsumoto, J. Non-Cryst. Solids, 290 (2001) 1-14.

[32] Y.H. Yun, P.J. Bray, J. Non-Cryst. Solids, 27 (1978) 363-380.

[33] M. Lenoir, A. Grandjean, Y. Linard, B. Cochain, D.R. Neuville, Chem. Geol., 256 (2008) 316-325.

[34] H. Miyoshi, D. Chen, H. Masui, T. Yazawa, T. Akai, J. Non-Cryst. Solids, 345-346 (2004) 99-103.

[35] M. Dapiaggi, G. Artioli, C. Righi, R. Carli, J. Non-Cryst. Solids, 353 (2007) 2852-2860.

[36] Z. Wang, Q.F. Shu, K.C. Chou, Metall. Mater. Trans. B, 44B (3) (2013) 606-613.

[37] H. Mizuno, H. Esaka, K. Shinozuka, M. Tamura, ISIJ Int., 48 (3) (2008) 277-285.

[38] P.W. McMillan, Glass-Cremics, Academic Press Inc. (London) LTD., London, 1964, p. 37-40.

[39] S. Mahadevan, A. Giridhar, A.K. Singh, J. Non-Cryst. Solids, 88 (1986) 11-34.

[40] A. Hruby, Czech. J. Phys. B, 22 (11) (1972) 1187-1193.

[41] Y. Cheng, H.N. Xiao, W.M. Guo, W.M. Guo, Thermochim. Acta, 444 (2) (2006) 173-178.

[42] T. J. Ahrens, Mineral Physics and Crystallography: A Handbook of Physical Constants, American Geophysical Union, Washington, 1995, p.64.

KRISTALIZACIONE KARAKTERISTIKE STAKLASTOG LIVNOG PRAHA UZ PRISUSTVO B₂O₃ I TiO₂ KOJI NE SADRŽI FLUORIDE

Z. Wang [a, b, c, d, *], Q.-F. Shu [e], K.-C. Chou [e]

[a*] Institut za procesnu tehniku, Kineska akademija nauka, Glavna laboratorija za složene multifazne sisteme, Peking, Kina

[b*] Univerzitet kineske akademije nauka, Fakultet za hemijsko inženjerstvo, Peking, Kina

[c*] IPE institut za proizvodnju u zelenoj industriji u nanđingu, Nanđing, Kina

[d*] Akademija za inovaciju u zelenoj proizvodnji, Kineska akademija nauka, Peking, Kina

[e] Univerzitet za nauku i tehnologiju u Pekingu, Glavna laboratorija za naprednu metalurgiju, Peking, Kina

Apstrakt

Da bi se ispitao uticaj TiO_2 i/ili B_2O_3 na kristalizaciju sloja šljake koji ne sadrži fluoride u blizini bakarnog kalupa, kristalizacione karakteristike livnog praha koji umesto fluorida sadrži TiO_2 i/ili B_2O_3 ispitane su XRD, SEM i DTA tehnikom. Indeks sposobnosti formiranja stakla (Kgl) je ispitan pomoću Harbijeve metode. XRD i SEM analize su pokazale da su $Ca_2Al_2SiO_7$, $CaTiO_3$ i $CaSiO_3$ dominantni kristali u ovom sistemu. Kada se sadržaj TiO_2 povećava od 0 do 7%, kristalizacija $Ca_2Al_2SiO_7$ i CaSiO3 se inhibira, dok je formiranje $CaTiO_3$ slabo, što ukazuje da tendencija kristalizacije livnog praha koji ne sadrži fluoride takođe slabi. Međutim, kada sadržaj TiO_2 dostigne 10%, tendencija kristalizacije jača zbog jake kristalizacije $CaTiO_3$. Povećanje sadržaja B_2O_3 inhibira kristalizaciju kalcijum silikata, što slabi tendenciju kristalizacije livnog praha bez fluorida. Postupak kristalizacije ispitivanog livnog praha se podudara sa mehanizmom površinske kristalizacije. Ovo istraživanje pruža važne informacije za dalje istraživanje ponašanja prilikom trasfera toplote šljake koja sadrži TiO_2 i B_2O_3 i nalazi se između bakarnih kalupa i slaba da bi se ispitala korisnost livnih prahova sa sadržajem TiO_2 i B_2O_3 koji ne sadrže flouride.

Ključne reči: Livni prahovi bez fluorida; Kristalizacija; Šljaka; Indeks sposobnosti formiranja stakla; Kristalizacija na površini; TiO_2